Fluorescence Technique to Study Thickness Effect on Dissolution of Latex Films

ŞAZIYE UĞUR, ÖNDER PEKCAN

Department of Physics, Istanbul Technical University, Maslak 80626 Istanbul, Turkey

Received 12 July 1999; accepted 30 October 1999

ABSTRACT: In situ steady-state fluorescence (SSF) measurements were used for studying dissolution of Latex films in real time. Latex films with various thicknesses are formed from pyrene (P) labeled poly(methyl methacrylate) (PMMA) latex particles, sterically stabilized by polyisobutylene (PIB). Annealing of latex films were performed above T_g at 220°C temperature for 60 min. UV-Visible (UVV) spectrometer was used to measure the transparency of latex films. It was observed that thicker films formed more opaque films than thinner films. Heptane (20%), chloroform (80%) mixture was used as a dissolution agent. Diffusion of pyrene labeled PMMA chains was monitored in real time by the change of pyrene fluorescence intensity, I_P in the polymer-solvent mixture. Diffusion coefficients, D, and relaxation constants, k_0, of PMMA chains were measured and found to be strongly dependent on the latex films thicknesses**.** It is observed that thicker and opaque films dissolved much faster than the thinner and transparent films.
 J Appl Polym Sci 77: 1087–1095, 2000

Key words: fluorescence, latex film, thickness, dissolution, diffusion

INTRODUCTION

The term "latex film" normally refers to a film formed from soft latex particles where the forces accompanying the evaporation of water are sufficient to compress and deform the particles into a transparent, void-free film.[1,2] However, hard latex particles remain essentially discrete and undeformed during the drying process. Film formation from these dispersions can occur in several stages, as shown in Figure 1. In both cases, the first stage corresponds to the wet initial state. Evaporation of solvent leads to the second stage in which the particles form a close packed array; here if the particles are soft they are deformed to polyhedrons. Hard latexes, however, stay undeformed at this stage. Annealing of soft particles causes diffusion across particle-particle boundaries, which leads the film to a homogeneous continuous material. Annealing of hard latex particles however first leads to void closure[3,4] and after the voids disappear diffusion across particle-particle boundary starts, i.e., the mechanical properties of hard latex films can be evolved by annealing after all solvent has evaporated and all voids have disappeared.

The mechanism of polymer film dissolution is much more complicated than small molecule dissolution. The small molecule dissolution can be explained by Fick's law of diffusion with a unique diffusion rate.[5] However, in polymeric systems many anomalies or deviations from Fick's law of diffusion are observed,[6] particularly below the glass transition temperature of polymer. It has been well known that polymeric films dissolve mainly in three sequential steps as presented in Figure 2: Solvent penetration, polymer relaxation, and diffusion of polymer chains into the solvent reservoir.

In the last decade it has become possible to observe latex film formation at the molecular

Correspondence to: Ş. Uğur.

Journal of Applied Polymer Science, Vol. 77, 1087–1095 (2000)

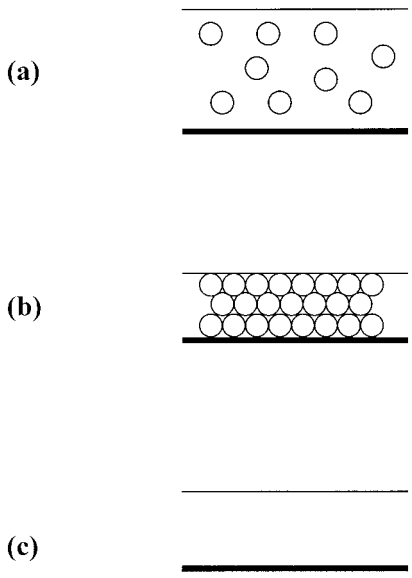

Figure 1 Stages of film formation from latex particles. (a) dispersion, (b) close packed particles after evaporation, (c) transparent film after annealing.

level. Polymer interdiffusion has been studied by direct nonradiative energy transfer (DET) using fluorescence decay measurements in conjunction with particles labeled with appropriate donor and acceptor chromophors.[7–10] These studies all indicate that in the particular systems examined, annealing the films above T_g leads to polymer interdiffusion at the particle-particle junction as the particle interface heals. Stephan Mazur[11] has written an extensive review on coalescence of polymer particles, where he mainly discusses the neck growth mechanism and its several geometrical approximations before interdiffusion of polymer chains takes place. Recently, the steady-state fluorescence and photon transmission techniques have been used in our laboratory to study void closure and interdiffusion processes during film formation from hard latex particles.[12–15]

Poly(methyl methacrylate) (PMMA) film dissolution was first studied using laser interferometry by varying molecular weight and solvent quality.[16] The interferometric technique was used to study dissolution of fluorescence labeled PMMA films. By monitoring the intensity of fluorescence from the film along with the interferometric signal, the solvent penetration rate into the film and the dissolution were measured simultaneously.[17] A real-time, nondestructive method for monitoring small molecules diffusion in polymer films was developed.[18–20] This method is essentially based on the detection of excited fluorescence dyes diffusing out of a polymer film into a solution in which the film is placed. Recently, we have reported a steady-state fluorescence (SSF) study on dissolution of both annealed hard latex films and PMMA discs using real-time monitoring of fluorescence probes.[21–24] In these studies effect of stirring, temperature, and solvent quality has been studied and second and last steps of polymer dissolution were investigated.

In this work various films formed from PMMA particles labeled with pyrene (P) with different latex content were prepared and annealed at 220°C in 60 min. Transmitted light intensity, I_{tr} from annealed latex films were measured by UV-Visible (UVV) technique to study the thickness effect on latex film formation. It is observed that I_{tr} obeyed Lambert's law.

Chloroform (80%) -heptane (20%) mixture was used as dissolution agents for latex film dissolution. SSF experiments were performed for the films with various thicknesses in real time monitoring of the dissolution process. The dissolution experiments were designed so that P labeled PMMA chains, diffusing from swollen gel were

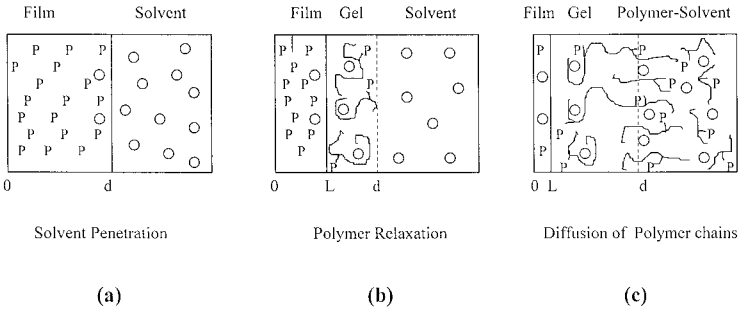

Figure 2 Polymeric film dissolution. (a) solvent penetration into film, (b) polymer chain relaxation in swollen gel, (c) diffusion of polymer chains into solvent reservoir.

Table I

$d(\mu m)$	Desorption Coefficient $D \times 10^{-10}$ ($cm^2\ s^{-1}$)	Relaxation Constant $k_0 \times 10^{-1}$ ($mg/cm^2\ min$)
10	3.7	—
20	5.2	4.1
30	81.5	4.5
40	41	9.2
50	176.3	8.36
60	64.6	8.33
80	870	—
100	795.7	17.71

detected by the fluorescence intensity of P. The goal of the presented work is to prepare mechanically strong films with various thicknesses, and then study the effect of packing on dissolution processes. It is observed that thicker film dissolved much faster than the others. Diffusion coefficients, D were measured in between 3×10^{-10} to $8 \times 10^{-8}\ cm^2\ s^{-1}$ from thinnest to thickest film samples.

EXPERIMENTAL

Latex Film Formation

PMMA-Polyisobutylene (PIB) polymer particles were prepared separately in a two-step process. First MMA was polymerized to low conversion in cyclohexane in the presence of PIB containing 2% isoprene units to promote grafting. The graft copolymer produced served as dispersant in the second stage of polymerization, in which MMA was polymerized in a cyclohexane solution of the polymer. In this stage PMMA chains are labeled covalently with pyrene groups. Details have been published elsewhere.[28] A stable dispersion of spherical polymer particles was produced, ranging in radius from 1 to 3 μm. A combination of ^{1}H-NMR and UV analysis indicated that these particles contain 4 mol % PIB and 3 mol % pyrene. (These particles were prepared by B. Williamson in Prof. M. A. Winnik's Laboratory in Toronto, Canada.)

Latex film preparation was carried out in following manner. Latex particles were dispersed in heptane in a test tube with 20% solid content. Eight different film samples with different thicknesses were prepared from this dispersion, by placing various number of drops on a glass plates with the size of $2.5 \times 0.8\ cm^2$. The heptane was allowed to evaporate. Then the films were annealed above the glass transition temperature of PMMA for 60 min at 220°C. During annealing, temperature was maintained within ±2°C. Samples were weighed before and after the casting to determine the latex contents and film thicknesses. These values are summarized in Table I. The average size of the particles was taken as 2 μm to calculate the thickness of the films. UVV experiments for latex film formation were carried out with the model Lambda 2 UV-Visible spectrometer of Perkin Elmer and transmitted light intensity, I_{tr}, was detected between 330 and 400 nm as seen in Figure 3 for the films with different thicknesses.

Film Dissolution

Dissolution experiments were performed in a 1.0 × 1.0 cm quartz cell that was placed in the spectrofluorimeter (Perkin Elmer LS50). Fluorescence emission intensity was monitored at 90° angle so that film samples were not illuminated by the excitation light. Film samples were attached at one side of quartz cell filled with chloroform (80%)-heptane (20%) mixture. The cell was then illuminated with 345 nm excitation light. Pyrene fluorescence intensity, I_p, was monitored during the dissolution process at 395 nm using the "time drive" mode of spectrofluorimeter. Emission of P-labeled polymer chains was recorded continuously at 395 nm as a function of time until there was no observable change in intensity. The disso-

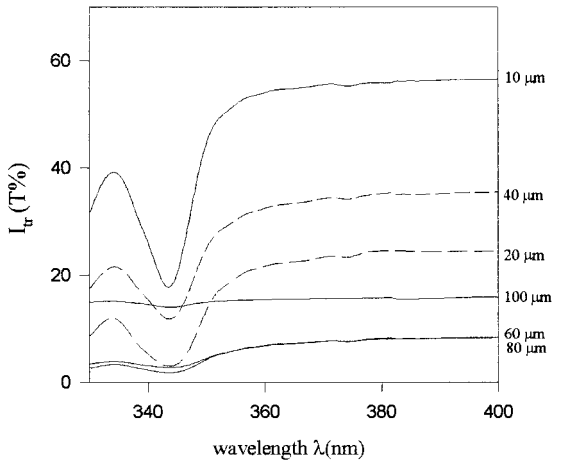

Figure 3 The plots of transmitted light intensity, I_{tr}, versus wavelength for the film samples in various thicknesses.

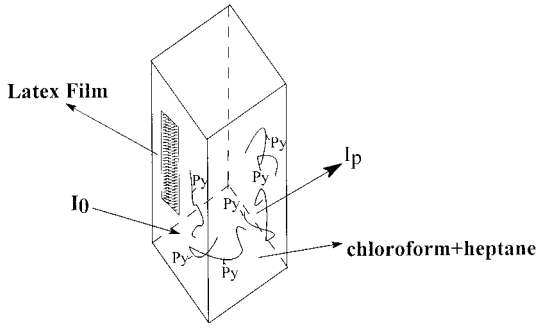

Figure 4 The cartoon representation of the dissolution cell and the film position in the spectrofluorimeter.

lution cell and the film position is presented in Figure 4. Eight different dissolution experiments were run for the films with different thicknesses.

RESULTS AND DISCUSSION

Opacity of Latex Films

Transmitted light intensity, I_{tr}, at 400 nm is plotted versus film thicknesses in Figure 5 for eight different latex films. It is seen that I_{tr} decreases as film thickness is increased. In other words when the latex film is formed and annealed it goes from opaque to transparent state. Usually the opacity of a medium is created by the scattering of the light. If the intensity of incident light is I_0, and on passage of the light through a medium of thickness d the incident intensity is reduced to I_{tr} as a result of scattering, then the opacity of the medium is determined by the following equation

$$\frac{I_{tr}}{I_0} = \exp(-\tau d) \qquad (1)$$

which is called Lambert's equation. Where opacity τ is defined as the fraction of primary light beam scattered in all directions on passage through a medium with thickness of 1 cm.

The expression I_{tr}/I_0 has been known as the light transmission or relative transparency. In general opacity is given by $\tau = (\varepsilon + \kappa)c$, where ε and c are the molar absorption coefficient and molar concentration, respectively. κ is known as imaginary absorption coefficient. ε is usually depends on the wavelength of the light being observed, temperature, and nature of the medium. κ presents the true absorption of light, i.e., when light is absorbed by a system its energy is transformed into thermal or electronic energy. The molar absorption coefficient, κ does not include the size of particles if they exist in the medium. It is known that the size of particles affects light absorption indirectly through either light scattering or reflection. In general light is scattered only when its wavelength is greater than the size of a particle in the medium. If the wavelength of the light is much smaller than the particle diameter, light is reflected. When the size of particles becomes considerably greater than λ, light is no more scattered but reflected, regardless of the light wavelength. If the particles are too large, light reflection from them increases which causes the reduction of the intensity of scattered light. The fact is that, as a result of light scattering, the white light that passes through a medium still loses some radiation in the short wavelength region that is not the true absorption. Such absorption is known as the imaginary absorption that is identified with κ, which is a function of particle size. If $\varepsilon = 0$ the system has no true absorption.

In our experiments, because the latex films annealed at 220°C for 60 min, it is believed that no voids between latex particles can exist, i.e., at 220°C PMMA as bulk reaches a melting state and flows easily by filling up the voids. Here opacity of the thicker films may be explained by the existing of cracks or pores in the latex film due to high packing. The size of these cracks and pores can be either larger or smaller than the wavelength of the light that result either reflection or scattering of light from the film, where both causes the reduction of transmitted light intensity, I_{tr}, according to eq. (1). In our experiments it is assumed that films has no true absorption for the wave-

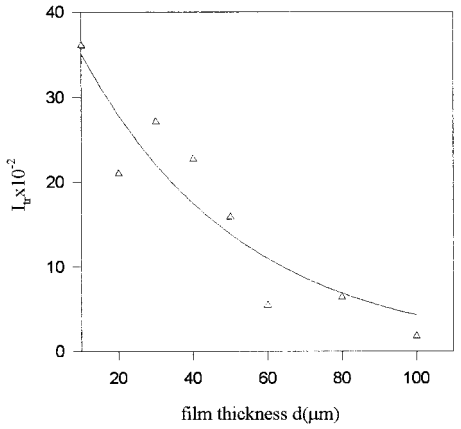

Figure 5 The plots of I_{tr} at 400 nm versus film thicknesses.

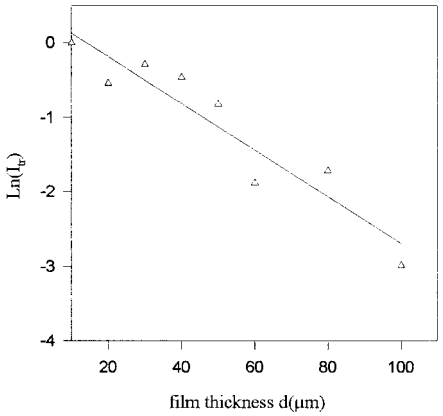

Figure 6 The fit of the data in Figure 5 to eq. (1). The slope of the linear relation produces the absorption coefficient μ as 314 cm^{-1}.

lengths of greater than 360 nm, i.e., it is believed that latex film either scatters or reflects light. But does not make true absorption at these wavelengths.

The data in Figure 5 are fitted to the logarithmic form of eq. (1) and plotted in Figure 6. The slope of the linear relation in Figure 6 produced κ value as 314 cm^{-1} where it is assumed that $\varepsilon = 0$.

Modeling of Dissolution

During in situ dissolution experiments, P labeled polymer chains were excited at 345 nm where latex film make true absorption and the variation in fluorescence emission intensity, I_P, was monitored with the "time drive" mode of spectrofluorimeter. Figure 7 presents the P intensities, I_P, as a function of "dissolution time, t_d" for film samples in various thicknesses listed in Table I. These curves reach a plateau almost in the same fashion at long times. In order to quantify the curves in Figure 7 various models can be proposed. In general polymeric films dissolve mainly in three different stages: (a) solvent diffusion, (b) polymer relaxation, and (c) desorption of polymer chains into the solvent reservoir. A schematic representation of these three sequential steps for the dissolution of a polymer film is presented in Figure 2. In the first stage, the penetration distance of solvent molecules mainly depends on free volume, which in turn depends on the flexibility of the chains, backbone, and side groups, as well as the thermal history of the polymer. These first solvent molecules act as a plasticizer and as a result these regions of the film start to swell. In the second stage, a gel layer is created by the relaxing polymer chains. This transition layer is composed of both polymer chains and solvent molecules. If the solvent–polymer interactions (solubility) are more dominant than polymer–polymer interaction, maximum swelling is obtained. This is the case when the good solvent is used during dissolution of a polymer film. In the last stage chain disentanglement takes place, chains separate from the bulk and desorb into the solvent.

Tu and Quano[25] proposed a model that includes polymer diffusion in a liquid layer adjacent to the polymer and moving of the liquid-polymer boundary. The key parameter for this model was the polymer disassociation rate, defined as the rate at which polymer chains desorb from the gel interface. Later Astarita and Sarti[26] proposed a model that takes glassy to swollen transition kinetics explicitly into account. Lee and Peppas[27] extended Tu and Quano's model for films to the situations of the polymer dissolution rate where gel thickness was found to be proportional to $(\text{time})^{1/2}$. A relaxation controlled model was proposed by Brochard and de Gennes[28] where, after a swelling gel layer was formed, desorption of polymer from the swollen bulk was governed by the relaxation rate of the polymer stress. This rate was found to be of the same order of magnitude as the reptation time. The dependencies of the radius of gyration and the reptation time on polymer molecular weight and concentration were studied, using a scaling law,[29] based on the reptation model.

In this work we found it appropriate to use the model developed by Enscore et. Al.[30] to interpret

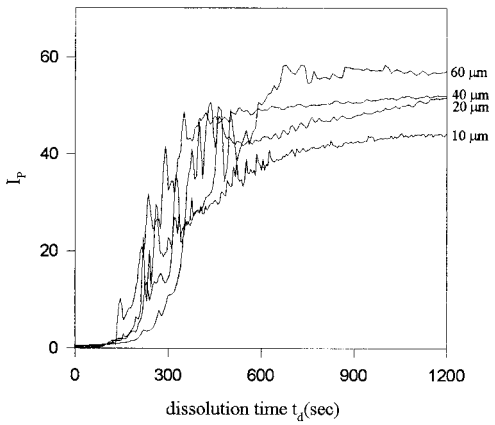

Figure 7 Pyrene intensities, I_P, versus dissolution time, t_d, for the film samples dissolved in chloroform-heptane mixture. Number on each dissolution curve indicates the film thicknesses in μm.

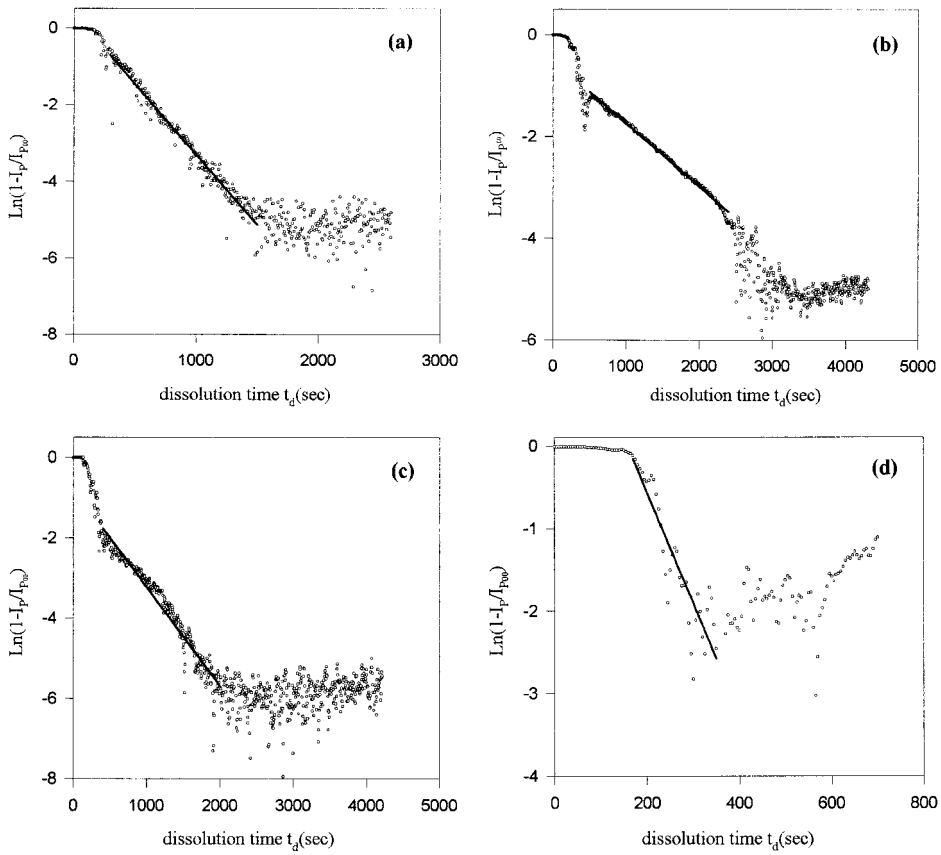

Figure 8 The fit of the dissolution data at intermediate region according to eq. (8) for the film samples in various thicknesses: (a) 10, (b) 20, (c) 40, and (d) 80 μm. Slope of the curves produce diffusion coefficients D, which are listed in Table I.

the results of film dissolution experiments. This model includes Case I and Case II diffusion kinetics, which are described below.

When the diffusion equation is solved in one dimension for a constant diffusion coefficient, D and fixed boundary conditions, the sorption and desorption transport in and out of a thin slab is obtained and given by the following relation[5]:

$$\frac{M_t}{M_\infty} = 1 - \frac{8}{\pi^2} \sum_{n=0}^{\infty} \frac{1}{(2n+1)^2} \exp\left(\frac{-(2n+1)^2 D\pi^2 t}{d^2}\right) \tag{2}$$

Here, M_t represents the amount of materials absorbed or desorbed at time t, $M\infty$ is the equilibrium amount of material, and d is the thickness of slab. Equation (2) presents the model for Case I diffusion, generally known as Fickian diffusion.

The mechanism of Case II diffusion is characterized by the following steps. As the solvent molecules enter into the polymer film, a sharp advancing boundary forms and separates the glassy part of the film from the swollen gel (see Fig. 2b). This boundary moves into the film at a constant velocity. The swollen gel behind the advancing front is always at a uniform state of swelling. Now, consider a cross-section of a film with thickness d, undergoing Case II diffusion as in Figure 2, where L is the position of the advancing sorption front, C_0 is the equilibrium penetrant concentration and k_0 (mg/cm^2 min) is defined as the Case II relaxation constant. The kinetic expression for the sorption in the film slab of an area A is given by

$$\frac{dM_t}{dt} = k_0 A \tag{3}$$

The amount of penetrant, M_t absorbed in time t will be

$$M_t = C_0 A(d - L) \tag{4}$$

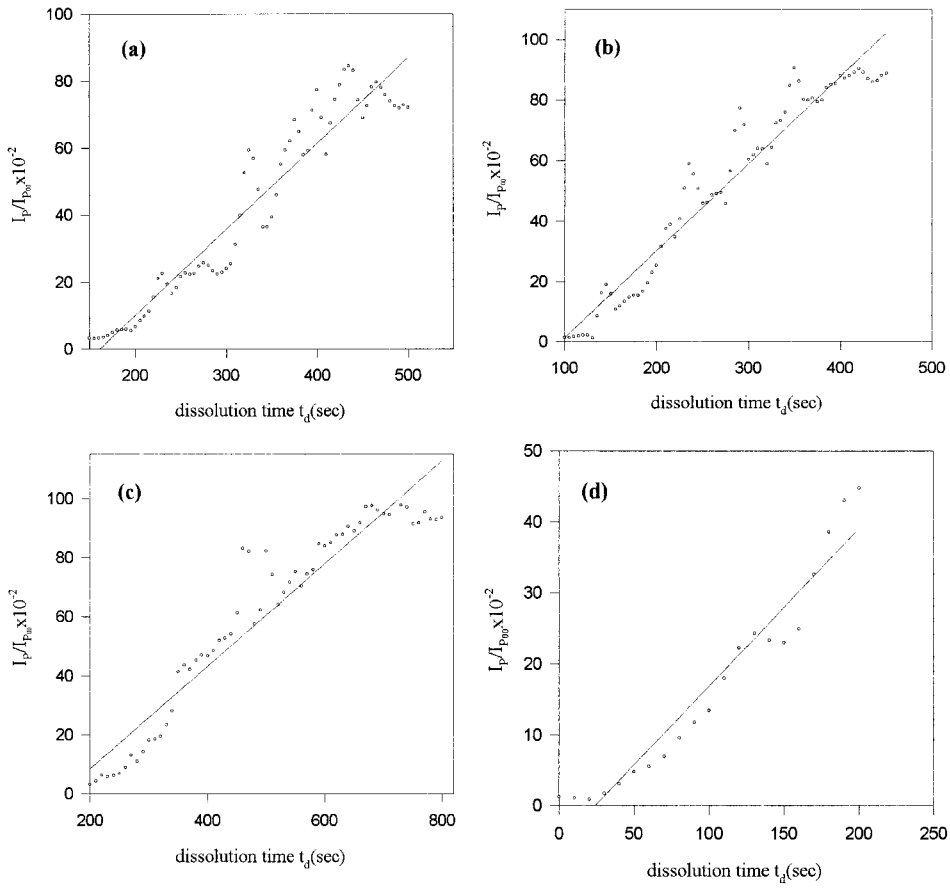

Figure 9 The fit of the dissolution data at early times according to eq. (9) for the film samples in various thicknesses: (a) 20, (b) 40, (c) 60, and (d) 100μm. Slope of the curves produce relaxation constant, k_0, which are listed in Table I.

After eq. (4) is substituted into eq. (3) the following relation is obtained:

$$\frac{dL}{dt} = -\frac{k_0}{C_0} \tag{5}$$

It can be seen that the relaxation front, positioned at L, moves toward the origin with a constant velocity, k_0/C_0. The algebraic relation for L, as a function of time t, is described by eq. (6):

$$L = d - \frac{k_0}{C_0}\, t \tag{6}$$

Because $M_t = k_0At$ and $M\infty = C_0Ad$, the following relation is obtained:

$$\frac{M_t}{M_\infty} = \frac{k_0}{C_0 d}\, t \tag{7}$$

The dissolution curves, in Figure 7, can be quantified by fitting the data to eq. (2). Figure 8a–d present the plot of the following relation, for film samples in various thicknesses, respectively.

$$Ln\left(1 - \frac{I_p}{I_{p\infty}}\right) = B - At \tag{8}$$

This is the logarithmic form of eq. (2) for n = 0 with $A = D\pi^2/d^2$ and $B = Ln(8/\pi^2)$ parameters. Here, it is assumed that I_p is proportional to the number of P labeled chains desorbing from the latex film and $I_{p\infty}$ presents its value at the equilibrium condition. In Figure 8 all dissolution curves are digitized for numerical treatment. Deviations from the linearity in Figure 8a–d at long times present equilibration of the dissolution process. Linear regions of the curves at intermediate times in Figure 8a–d follow the Fickian diffusion model. When the linear portions of the curves in

Figure 8a–d are compared with computations using eq. (8), chain desorption coefficients, D are obtained and are listed in Table I. When one compares the observed D $\approx 10^{-10} - 10^{-8}$ cm^2/s values with the backbone diffusion coefficient of interdiffusing polymer chains during film formation from PMMA latex particles,[30,31] ($\approx 10^{-16} - 10^{-14}$ cm^2/s) 6 to 4 orders of magnitude difference can be seen. This is reasonable for the chains desorbing from swollen gel, during dissolution of PMMA latex films.

Non-Fickian behavior of the curves short time region in Figure 9a–d can be interpreted by using eq. (7). When $I_p/I_{p\infty}$ are plotted as a function of dissolution time, t_d, reasonable linear fits were obtained for the curves in Figure 9. If we assume that the amount of solvent molecules is proportional to the number of PMMA chains desorbing from the swollen gel, than eq. (7) can be written as

$$\frac{I_P}{I_{P\infty}} = \frac{k_0}{C_0 d}\, t \tag{9}$$

Fitting eq. (9) to the data presented in Figure 9 yielded k_0 parameter. Using known d and C_0 (1.33 g/mL) values, k_0 parameters were obtained and listed in Table I. The measured k_0 values are resulted three orders of magnitude difference from those of Stannet and Hopfenberg.[30,31] Thus, for n-hexane sorption by polystyrene spheres and film they reported k_0 around 10^{-5} mg/cm^2min. This difference can be caused by the stronger solvent-polymer interaction in our solvent-PMMA system.

The plots of D and k_0 versus film thickness, d, are presented in Figure 10a,b, where it is seen that diffusion coefficient and relaxation constant obey the following relations, respectively:

$$D = D_0 \exp(\alpha d) \tag{10}$$

$$k_0 = k_{10} + \beta d \tag{11}$$

Here α and β are the related constants and D_0 and k_{10} are the diffusion coefficient and the relaxation constant at d = 0. The logarithmic plot of eq. (10) is given in Figure 11, which presents a nice linear relation by indicating that the thickness dependence of D obeys the relation in eq. (10). On the other hand relaxation constant, k_0 satisfies the linear dependence on d.

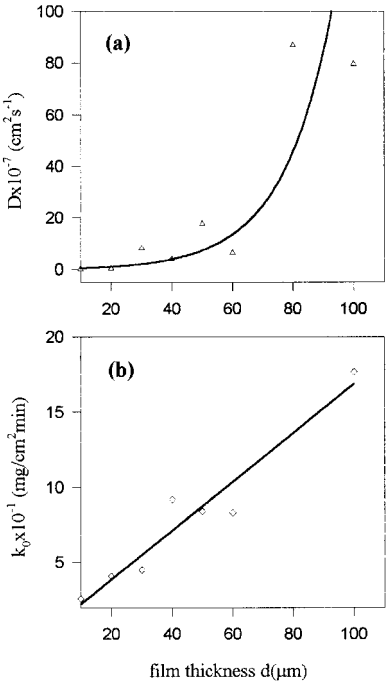

Figure 10 The plot of D (a) and k_0 (b) versus film thickness, d.

CONCLUSION

In previous sections opacity of the latex films are related to the pores and cracks created in thicker films during annealing. These pores and cracks are imperfections created due to high packing of latex particles in thicker films, which may cause high dissolution rates. In other words pores and cracks increase the surface area in films against solvent molecules and as result thicker films dis-

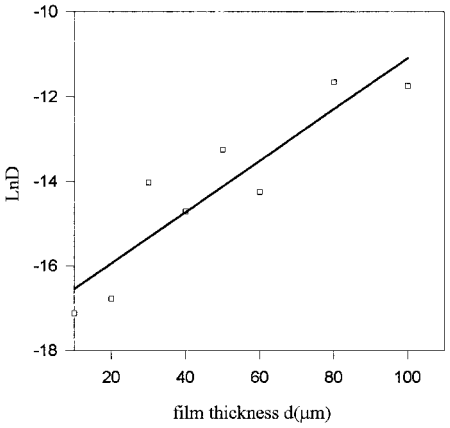

Figure 11 The plot of eq. (10), which obeys the data in Figure 10a.

solve faster. In order to quantify the above argument thickness of the film, d has to be related to the number of pores and cracks in eqs. (10) and (11) as follows:

$$D = D_0 \mathbf{exp}(\alpha_0 n) \tag{12}$$

$$k_0 = k_{10} + \beta_0 n \tag{13}$$

where α_0 and β_0 are the related constants and n is number of pores and cracks per unit volume in the film. Equations (12) and (13) predict that films with high n have larger relaxation constants and diffusion coefficients due to easier penetration of solvent molecules into the pores films. Equations (12) and (13) can be considered to be the modifications of the case I and case II diffusion kinetics for the thin slap model.

REFERENCES

1. Eckersley, S. T.; Rudin, A. J Coatings Technol 1990, 62, No 780, 89.
2. Joanicot, M.; Wong, K.; Maquet, J.; Chevalier, Y.; Pichot, C.; Graillat, C.; Linder, P.; Rios, L.; Cabane, B. Prog Coll Polym Sci 1990, 81, 175.
3. Sperry, P. R.; Snyder, B. S.; O'Down, M. L.; Lesko, P. M. Langmuir 1994, 10, 2619.
4. Mackenzie, J. K.; Shutlewort, R. Proc Phys Soc 1949, 62, 838.
5. Crank, J. The Mathematics of Diffusion; Oxford: Clarendon Press, 1975.
6. Crank, J.; Park, G. S. Diffusion in Polymer; Acad. Press: London, 1968.
7. Pekcan, Ö.; Winnik, M. A.; Croucher, M. D. Macromolecules 1990, 23, 2673.
8. Zhao, C. L.; Wang, Y.; Hruska, Z.; Winnik, M. A. Macromolecules 1990, 23, 4082.
9. Wang, Y.; Zhao, C. L.; Winnik, M. A. J Chem Phys 1991, 95, 2143.
10. Boczar, E. M.; Dionne, B. C.; Fu, Z.; Kirk, A. B.; Lesko, P. M.; Koller, A. D. Macromolecules 1993, 26, 5772.
11. Mazur, S. Coalescence of Polymer Particles. In Polymer Powder Technology; Maukis, M.; Rosenweig, V., Eds.; John Wiley and Sons: New York, 1996.
12. Canpolat, M.; Pekcan, Ö. Polymer 1995, 36, 4433.
13. Canpolat, M.; Pekcan, Ö. Polymer 1995, 36, 2025.
14. Pekcan, Ö.; Erda, E.; Kesenci, K.; Piþkin, E. J Appl Polym Sci 1998, 68, 1257.
15. Pekcan, Ö.; Erda, E. J Appl Polym Sci 1998, 70, 339.
16. Krasicky, P. D.; Groele, R. J.; Rodriguez, F. J Appl Polym Sci 1988, 35, 641.
17. Limm, W.; Dimnik, G. D.; Stanton, D.; Winnik, M. A.; Smith, B. A. J Appl Polym Sci 1988, 35, 2099.
18. Pascal, D.; Duhamel, J.; Wang, Y.; Winnik, M. A.; Napper, D. H.; Gilbert, R. Polymer 1994, 34, 1134.
19. Lu, L.; Weiss, R. G. Macromolecules 1994, 27, 219.
20. Krongauz, V. V.; Mooney, III, W. F.; Palmer, J. W.; Patricia, J. J. J Appl Polym Sci 1995, 56, 1077.
21. Pekcan, Ö.; Canpolat, M.; Kaya, D. J Appl Polym Sci 1996, 60, 2105.
22. Pekcan, Ö.; Ugur, Ş.; Yilmaz, Y. Polymer 1997, 38, 2183.
23. Ugur, Ş.; Pekcan, Ö. Polymer 1997, 38, 5579.
24. Pekcan, Ö.; Ugur, Ş. J Appl Polym Sci 1998, 70, 1493.
25. Tu, Y. O.; Quano, A. C. IBM, J Res D 1977, 21, 131.
26. Astaria, G.; Sarti, G. C. Polym Eng Sci 1978, 18, 388.
27. Lee, P. I.; Peppas, N. A. J Controlled Release 1987, 6, 207.
28. Brochard, F.; de Gennes, P. G. Phycico Chem Hydrodynamics 1983, 4, 313.
29. Papanu, J. S.; Soane, D. S.; Bell, A. T. J Appl Polym Sci 1989, 38, 859.
30. Enscore, D. J.; Hopfenberg, H. B.; Stannett, V. T. Polymer 1977, 18, 793.
31. Jacques, C. H. M.; Hopfenberg, H. B. Polym Eng Sci 1974, 14, 449.